

# Efficient generative adversarial networks using linear additive-attention Transformers

Emilio Morales-Juarez and Gibran Fuentes-Pineda

**Abstract**—Although the capacity of deep generative models for image generation, such as Diffusion Models (DMs) and Generative Adversarial Networks (GANs), has dramatically improved in recent years, much of their success can be attributed to computationally expensive architectures. This has limited their adoption and use to research laboratories and companies with large resources, while significantly raising the carbon footprint for training, fine-tuning, and inference. In this work, we present LadaGAN, an efficient generative adversarial network that is built upon a novel Transformer block named Ladaformer. The main component of this block is a linear additive-attention mechanism that computes a single attention vector per head instead of the quadratic dot-product attention. We employ Ladaformer in both the generator and discriminator, which reduces the computational complexity and overcomes the training instabilities often associated with Transformer GANs. LadaGAN consistently outperforms existing convolutional and Transformer GANs on benchmark datasets at different resolutions while being significantly more efficient. Moreover, LadaGAN shows competitive performance compared to state-of-the-art multi-step generative models (e.g. DMs) using orders of magnitude less computational resources<sup>1</sup>.

**Index Terms**—image generation, GAN, linear additive-attention, efficient Transformer

## I. INTRODUCTION

Generative Adversarial Networks (GANs) [1] have been one of the preferred approaches to image generation over the past decade [2], [3]. A key benefit of GANs lies in their ability to learn a smooth and continuous latent space representation of the data. This latent space allows for intuitive manipulation of the generated samples, such as smoothly transitioning between different samples and performing arithmetic operations on the latent vectors. Although diffusion models [4] have recently outperformed GANs in different generation tasks, they require multiple forward passes to generate a single sample, which translates into large computational resources. In contrast, GANs can generate samples in a single forward pass without additional training procedures, such as progressive distillation [5]. Moreover, some results suggest that GANs can match the quality of diffusion models (DM) using smaller networks (e.g. ADM-IP [6] with 296 million parameters and VITGAN [7] with 38 million parameters achieve a similar performance on CelebA).

Training instability is a challenge that has limited the application and adoption of GANs. Standard techniques to

tackle this issue propose different objective functions (e.g. Wasserstein distance [8]) and regularization techniques (e.g. spectral normalization [9]). Moreover, laborious engineering and sophisticated neural modules [10], [11] are required to achieve state-of-the-art image generation using Conv-based GANs, resulting in computationally demanding architectures (e.g. StyleGANs [10], [11]) regarding parameters and FLOPs. Since the inductive bias of convolutions has been shown to limit long-range dependency learning [12], different GAN architectures that incorporate Transformers [13] have been proposed. However, self-attention can make GAN training even more unstable [7], and its  $O(N^2)$  complexity results in high computational demands [7], [14].

This paper presents LadaGAN, an efficient GAN architecture for image generation that is based on linear additive-attention Transformers, which we call Ladaformer. This LadaGAN block is inspired by Fastformer [15], an architecture originally proposed for text processing. We employ Ladaformer in both the generator and the discriminator of LadaGAN, allowing efficient processing of long sequences in both networks. In the generator, this block progressively generates a global image structure from the latent space using attention maps. In the discriminator, the Ladaformer generates attention maps to distinguish real and fake images. Notably, the design of LadaGAN reduces the computational complexity and overcomes the training instabilities often associated with Transformer GANs.

We exhaustively evaluate the proposed model with different resolutions of CIFAR-10, CelebA, FFHQ, and LSUN Bedroom. LadaGAN achieves a competitive FID score compared with state-of-the-art GANs, ADM-IP and CT on all these datasets, while requiring significantly fewer FLOPs and parameters. In order to validate the effectiveness of the proposed architecture, we evaluate various  $O(N)$  attention mechanisms with gradient penalty and their compatibility with the inductive bias of convolutions. Our findings indicate that the LadaGAN architecture is gradient-stable and its attention mechanism is convolution-compatible, thus proving to be a highly effective architecture for image generation.

## II. RELATED WORK

Motivated by the success achieved in natural language processing and image classification, transformer-based architectures have been proposed for GANs, showing competitive results compared to state-of-the-art convolutional models such as BigGAN [16] and StyleGANs [10], [11]. One of the first Transformer-based GANs was TransGAN [17], which employs gradient penalty [8], [18] to stabilize the training

E. Morales-Juarez is with the Facultad de Ingeniería, Universidad Nacional Autónoma de México, Mexico. Email: emilio.morales@fi.unam.edu.

G. Fuentes-Pineda is with the Instituto de Investigaciones en Matemáticas Aplicadas y en Sistemas, Universidad Nacional Autónoma de México, Mexico. Email: gibranfp@unam.mx.

<sup>1</sup>The source code is available at <https://github.com/milmor/LadaGAN>

of the transformer discriminator. TransGAN addresses the quadratic limitation using grid self-attention, which consists of partitioning the full-size feature map into several non-overlapping grids. TransGAN experiments have shown that grid self-attention achieves better results than Nyström [19] and Axis attention [20]. On the other hand, ViTGAN [7] generates patches, reducing the transformer output sequence length. To stabilize the transformer discriminator, this model employs L2 attention [21] and proposes a modification to the original spectral normalization [9]. Moreover, to improve performance, the generator uses implicit neural representations [22]. However, training both TransGAN and ViTGAN requires more than one GPU; TransGAN is trained on 16 V100 GPUs, and ViTGAN is trained on one TPU. Although the Swin-Transformer block has been explored in ViTGAN to reduce computational requirements, it underperforms the original Transformer block.

Because transformer discriminators have been found to affect the stability of adversarial training [7], more recent works have relied on conv-based discriminators, employing transformers only in the generator. For instance, HiT [23] is an architecture that addresses the quadratic complexity using multi-axis blocked self-attention. Similarly, the main block of StyleSwin’s generator [14] consists of a SwinTransformer. However, in addition to not taking advantage of transformers in the discriminator, the design of these architectures does not prioritize efficiency, so their training requires more than a single GPU; StyleSwin is trained on 8 32GB V100 GPUs, and HiT is trained on a TPU.

On the other hand, GANsformer [24] combines the inductive bias of self-attention and convolutions. This model consists of a bipartite graph and results in a generalization of StyleGAN, so it only partially takes advantage of the capacity of transformers. Combining convolutions and transformers has enhanced neural architectures in image classification tasks [25], [26], [27]; however, it has been less explored for image generation tasks. LadaGAN also combines convolutions and self-attention, but unlike GANsformer, it uses additive attention instead of dot-product attention, in both the discriminator and the generator, to tackle the quadratic complexity and training instability.

In the past years, diffusion models [28], [29] have outperformed GANs in several image generation tasks [30], [31]. This family of models learns to reverse a multi-step noising process, where each step requires a forward pass through the whole network. Among the most prominent diffusion models are DDPM (Denosing Diffusion Probabilistic Models) [29] and ADM (Ablated Diffusion Model) [31]. Nevertheless, these models are complex in terms of parameters and FLOPs, and multiple forward passes are required for generation, resulting in expensive training and inference. This has led to efforts to reduce the number of sampling steps [32], [29] for generation, including Consistency training (CT) [33], which has reduced the multi-step generation process to 2 steps. However, CT results in more expensive training than ADM (e.g. ADM-IP with 75M images and CT with 409M images achieve a similar performance on CIFAR-10) and underperforms it in terms of generation quality.

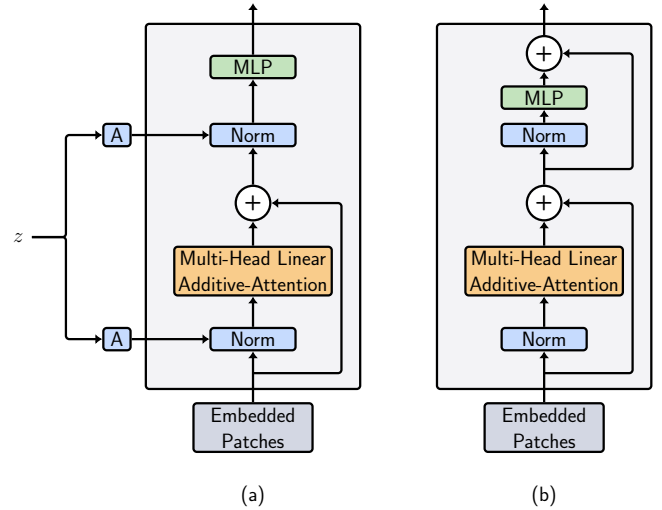


Fig. 1: Ladaformer: (a) generator with SLN and without MLP residual connection and (b) discriminator without SLN and with MLP residual connection.

### III. METHOD

#### A. Linear additive attention (Lada)

LadaGAN attention mechanism is heavily inspired by Fastformer’s [15] additive attention<sup>2</sup>. This efficient  $O(N)$  Transformer architecture was originally designed for text processing, achieving comparable long-text modeling performance to the original dot-product attention at a fraction of the computational cost. Instead of computing the pairwise interactions among the input sequence vectors, Fastformer’s additive attention creates a global vector summarizing the entire sequence using a single attention vector computed from the queries.

More specifically, this linear additive attention computes each weight by projecting the corresponding query vector  $\mathbf{q}_i \in \mathbb{R}^d$  with a vector  $\mathbf{w} \in \mathbb{R}^d$ , i.e.:

$$\alpha_i = \frac{\exp(\mathbf{w}^T \mathbf{q}_i / \sqrt{d})}{\sum_{j=1}^N \exp(\mathbf{w}^T \mathbf{q}_j / \sqrt{d})}. \quad (1)$$

where  $d$  is the head dimension.

To model interactions, a global vector is computed as follows:

$$\mathbf{g} = \sum_{i=1}^N \alpha_i \mathbf{q}_i. \quad (2)$$

An element-wise operation is performed between  $\mathbf{g}$  and each key vector  $\mathbf{k}_i \in \mathbb{R}^d$  to propagate the learned information, obtaining a vector  $\mathbf{p}_i \in \mathbb{R}^d$  such that

$$\mathbf{p}_i = \mathbf{g} \odot \mathbf{k}_i, \quad (3)$$

where the symbol  $\odot$  denotes element-wise product.

Unlike Fastformer [15], LadaGAN’s attention mechanism does not compute a global vector for the keys; instead, an element-wise operation is performed between each vector  $\mathbf{p}_i$

<sup>2</sup>Not to be confused with Bahdanau’s attention [34]

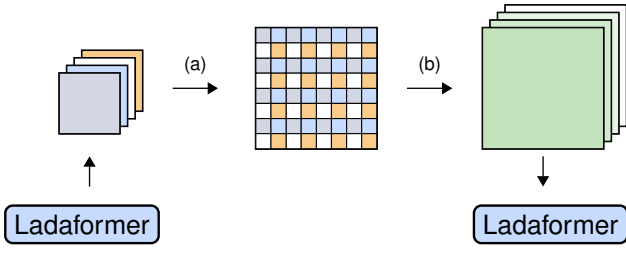


Fig. 2: Local Embedding Expansion. The output of the first Transformer consists of 4 feature maps that are expanded using pixel shuffle (a) to generate a single feature map. Then, the output map from pixel shuffle passes through a convolutional layer (b) to expand to 4 channels. These new 4 feature maps are the input to the second Transformer. In this way, even though the Transformers process sequences of different lengths, the dimensions of the embeddings are independent of the Pixel Shuffle operation.

and the corresponding value vector  $\mathbf{v}_i \in \mathbb{R}^d$ . This operation allows propagating the information of the attention weights  $\alpha_i, i = 1, \dots, N$  instead of compressing it. Finally, we compute each output vector  $\mathbf{r}_i \in \mathbb{R}^d$  as

$$\mathbf{r}_i = \mathbf{p}_i \odot \mathbf{v}_i. \quad (4)$$

### B. Ladaformer

The main block of the generator and discriminator is Ladaformer, which closely follows the Vision Transformer (ViT) architecture [12], as illustrated in Figure 1. However, since introducing self-modulation has shown to be an effective strategy to improve performance [35], [7], the LadaGAN generator block uses self-modulated layer normalization instead of standard layer normalization. In particular, layer normalization parameters for the inputs  $\mathbf{h}_\ell$  of the  $\ell$ -th layer are adapted by

$$\text{SLN}(\mathbf{h}_\ell, \mathbf{z}) = \gamma_\ell(\mathbf{z}) \odot \left( \frac{\mathbf{h}_\ell - \boldsymbol{\mu}}{\boldsymbol{\sigma}} \right) + \beta_\ell(\mathbf{z}), \quad (5)$$

where the division operation is performed element-wise.

Note that this is slightly different from ViTGAN’s self-modulated layer normalization, which injects a vector  $\mathbf{w}$  computed by passing the latent vector  $\mathbf{z}$  through a projection network; in contrast, LadaGAN injects  $\mathbf{z}$  directly. In addition, unlike ViT, ViTGAN, and Fastformer, the LadaGAN generator does not have the residual connection from the output of the attention module to the output of the multi-layer perceptron (MLP).

$$\mathbf{h}'_\ell = \text{MAA}(\text{SLN}(\mathbf{h}_{\ell-1}, \mathbf{z})) + \mathbf{h}_{\ell-1}, \quad (6)$$

$$\mathbf{h}_\ell = \text{MLP}(\text{SLN}(\mathbf{h}'_\ell, \mathbf{z})), \quad (7)$$

where  $\text{MAA}(\cdot)$  denotes the multi-head linear additive attention and  $\text{MLP}(\cdot)$  is a two-layer fully connected network with a GELU activation function in the first layer.

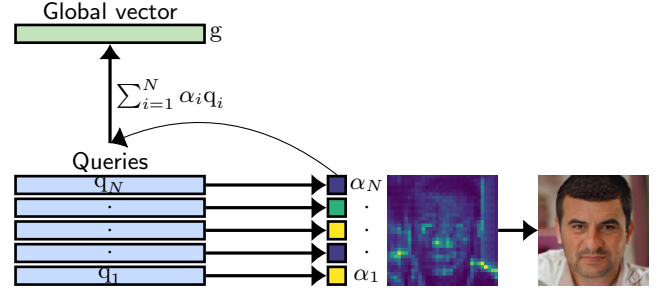


Fig. 3: Linear Additive Attention mechanism of a single head, generating a  $32 \times 32$  map to construct a global structure for the image. This process guides the generation of patches for  $128 \times 128$  image resolution.

### C. Generator

LadaGAN generator employs the pixel shuffle operation to progressively transform the latent vector into an image. This operation is a common technique to increase spatial resolution, in which the input is reshaped from  $(B, C \times r^2, H, W)$  to  $(B, C, H \times r, W \times r)$ , where  $r$  is a scaling factor,  $B$  is the batch size,  $C$  is the number of channels of the output and  $H$  and  $W$  are the height and width of the input. Although this technique was originally proposed as an efficient alternative to standard ConvNet-based upsampling in super-resolution architectures, it has been widely adopted in image generation Transformers, including recent Transformer GANs. Since a pixel shuffle operation reduces the number of channels  $C$  in the input (process (a) in Figure 2), we apply a convolutional layer after such operation to increase the number of channels; we denote this operation as Local Expansion of the Embedding

$$\text{LEE}(\mathbf{h}_\ell) = \text{Conv}(\text{PixelShuffle}(\mathbf{h}_\ell)) \quad (8)$$

where  $\text{Conv}(\cdot)$  is a standard convolutional layer with  $K$  filters and  $\text{PixelShuffle}(\cdot)$  denotes the pixel shuffle operation with  $r = 2$ .

LadaGAN generator uses the same architecture for the resolutions  $32 \times 32$ ,  $64 \times 64$ ,  $128 \times 128$ , and  $256 \times 256$ , which consists of three Ladaformer blocks, as shown in Figure 4 (a). Since increasing the sequence length of Transformer models has generally improved performance in natural language processing tasks, we posit that similar benefits can be obtained in image generation tasks. Therefore, taking advantage of the  $O(N)$  complexity of Ladaformer blocks, we aim to generate a long sequence (1024 tokens) as the output of the final Transformer block.

Given the latent vector  $\mathbf{z} \in \mathbb{R}^{D_z}$ , and  $L$  Transformer blocks, LadaGAN generator operates as follows:

$$\mathbf{h}_0 = \text{Linear}(\mathbf{z}), \quad (9)$$

$$\mathbf{h}'_\ell = \text{MAA}(\text{SLN}(\mathbf{h}_{\ell-1} + \mathbf{E}_{\ell-1}, \mathbf{z})) + \mathbf{h}_{\ell-1}, \quad (10)$$

$$\mathbf{h}_\ell = \text{LEE}(\text{MLP}(\text{SLN}(\mathbf{h}'_\ell, \mathbf{z}))), \quad (11)$$

$$\mathbf{y} = \text{MAA}(\text{SLN}(\mathbf{h}_L + \mathbf{E}_L, \mathbf{z})) + \mathbf{h}_L, \quad (12)$$

$$\mathbf{x} = \text{Conv}(\text{MLP}(\text{SLN}(\mathbf{y}, \mathbf{z}))), \quad (13)$$

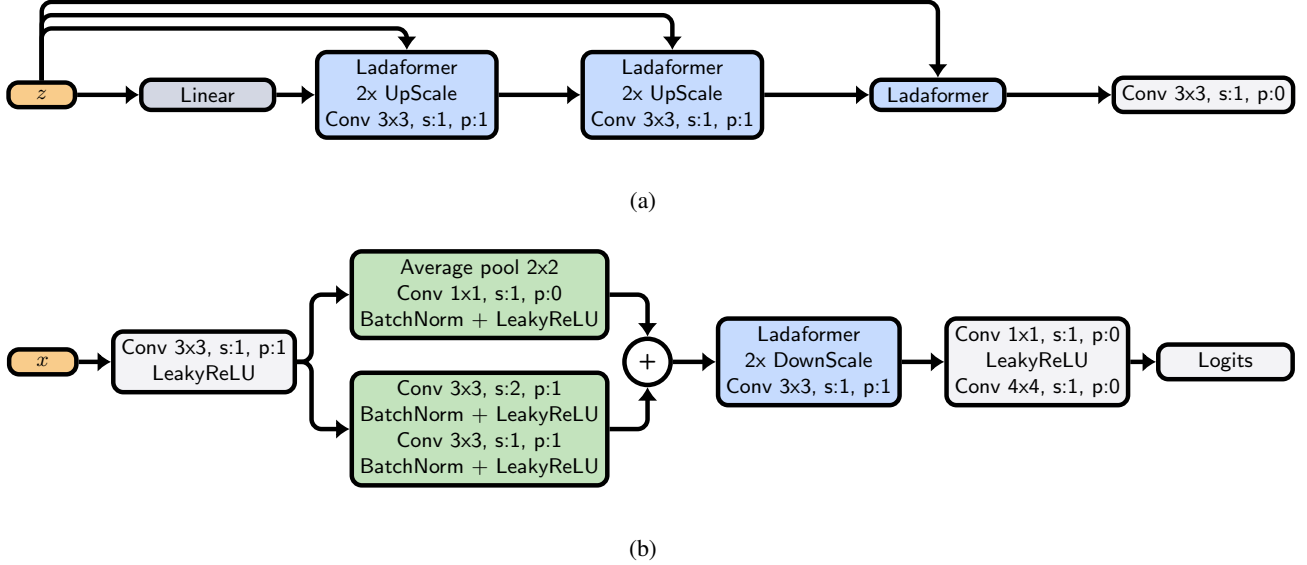


Fig. 4: LadaGAN architecture: Lada-Generator (a) and Lada-Discriminator (b).

where  $\ell = 1, \dots, L$ ,  $\text{Linear}(\cdot)$  denotes a linear projection,  $\mathbf{E}_L \in \mathbb{R}^{N_L \times D_L}$  and  $\mathbf{E}_{\ell-1} \in \mathbb{R}^{N_{\ell-1} \times D_{\ell-1}}$  are the positional embeddings for the blocks  $L$  and  $\ell - 1$  respectively, and  $\mathbf{x} \in \mathbb{R}^{H \times W \times C}$  is the output image. Note that before the final convolutional layer in equation 13 and every pixel shuffle operation, a reshape operation is performed to generate a 2D feature map. On the other hand, if the number of output channels of the LEE convolution in equation 11 is equal to the number of input channels, there is no expansion of the embedding dimension. This results in the convolution only reinforcing the pixel shuffle locality. Figure 3 shows the LadaGAN generative process.

#### D. Discriminator

LadaGAN discriminator resembles the FastGAN [36] discriminator but uses a Ladaformer instead of a residual convolutional block; the architecture of the LadaGAN discriminator is illustrated in Figure 4 (b). Lada compatibility with convolutions allows to have FastGAN-like residual blocks [36] as input to feed a Ladaformer. We found that combining the Ladaformer and FastGAN-like residual blocks [37] achieves stability. In particular, the batch normalization module [37] in the convolutional feature extractor proves to be essential to complement the stability of the Lada discriminator. Note that batch normalization is not typically employed by Transformer discriminators, such as ViTGAN and TransGAN.

In contrast to the LadaGAN generator, the discriminator Ladaformer block has the standard MLP residual connection, as shown in Figure 1 (b). In addition, a SpaceToDepth( $\cdot$ ) operation is performed at the output. As opposed to PixelShuffle( $\cdot$ ), SpaceToDepth( $\cdot$ ) down-sample the input by reshaping it from  $(B, C, H \times r, W \times r)$  to  $(B, C \times r^2, H, W)$ . Unlike the final layer of the TransGAN and ViT discriminators that uses the class embedding [38], the final layer of the LadaGAN discriminator consists of convolutions with strides of 2. In

this way, the convolutions progressively reduce the attention map representation.

#### E. Loss function

LadaGAN employs standard non-saturating logistic GAN loss with  $R_1$  gradient penalty [39]. The  $R_1$  term penalizes the gradient on real data, allowing the model to converge to a good solution. For this reason, it has been widely adopted in state-of-the-art GANs with convolutional discriminators. More specifically, the loss function is defined as follows:

$$\begin{aligned} \mathcal{L}_D = & -\mathbb{E}_{\mathbf{x} \sim P_{\mathbf{x}}} [\log(D(\mathbf{x}))] \\ & -\mathbb{E}_{\mathbf{z} \sim P_{\mathbf{z}}} [1 - \log(D(G(\mathbf{z})))] \\ & + \gamma \cdot \mathbb{E}_{\mathbf{x} \sim P_{\mathbf{x}}} [(\|\nabla_{\mathbf{x}} D(\mathbf{x})\|_2^2)], \end{aligned} \quad (14)$$

$$\mathcal{L}_G = -\mathbb{E}_{\mathbf{z} \sim P_{\mathbf{z}}} [\log(D(G(\mathbf{z})))]. \quad (15)$$

Note that the Lada stability allows training  $O(N)$  Transformer discriminators with  $R_1$  gradient penalty. This is particularly important since dot-product Transformer discriminators and  $R_1$  gradient penalty have been found to be incompatible [7], typically causing training instabilities.

## IV. EXPERIMENTS

To demonstrate LadaGAN stability, efficiency and competitive performance, we conduct an ablation study to assess the impact of the residual connections, convolutions, and modulation using different  $O(N)$  Transformers in the generator, as well as the behavior of a Lada discriminator. We also evaluate the efficiency of LadaGAN in terms of training data requirements. Finally, we compare the performance and computational complexity of LadaGAN with state-of-the-art single-step and multi-step image generation models.



TABLE I: FID and number of FLOPs for the LadaGAN generator using Linformer, Swin-Transformer, Fastformer, Ladaformer, and Lada-Swin attention mechanisms on CIFAR-10 ( $32 \times 32$ ).

Attention	Convolutions	Residual-MLP	Modulation	FLOPs	FID ↓	sFID ↓	IS ↑	Prec ↑	Rec ↑
Swin	✗	✓	✓	0.5B	7.96	5.21	8.91	0.55	0.57
Linformer	✗	✓	✓	0.6B	5.94	5.32	9.27	0.56	0.58
	✓	✓	✓	0.8B	6.59	5.21	9.10	0.56	<b>0.60</b>
	✓	✗	✓	0.8B	10.65	7.22	8.48	0.54	0.49
Fastformer	✗	✓	✓	0.4B	6.60	5.25	9.26	0.56	0.59
	✓	✓	✓	0.6B	6.57	5.31	9.32	<b>0.58</b>	0.56
	✓	✗	✓	0.6B	5.27	<b>4.48</b>	9.48	0.56	0.59
Lada-Swin	✗	✗	✓	0.4B	6.46	5.05	9.25	0.55	0.58
	✗	✓	✓	0.5B	6.47	5.76	9.24	0.56	0.58
Ladaformer	✗	✗	✓	0.5B	5.88	4.98	9.18	<b>0.58</b>	0.56
	✓	✓	✓	0.7B	6.29	5.43	9.26	0.57	0.57
	✓	✗	✓	0.7B	<b>4.82</b>	4.57	<b>9.69</b>	<b>0.58</b>	0.59
	✓	✓	✗	0.7B	6.19	6.28	9.35	0.57	0.57
	✓	✗	✗	0.7B	5.87	4.73	9.33	0.57	0.53

### A. Experiment setup

We perform experiments on four widely used datasets for image generation, namely CIFAR-10 [40], CelebA [41], FFHQ [11], and LSUN bedroom [42]. CIFAR-10 consists of 60k  $32 \times 32$  images of 10 different classes, which is divided into 50k training images and 10k test images. CelebA is composed of 182,732 images of human faces with a resolution of  $178 \times 218$ ; this dataset is split into 162,770 for training and 19,962 for testing. We resize all CelebA images to  $64 \times 64$ . Here, we use the *aligned* version of CelebA, which is different from the *cropped* version. FFHQ is a dataset of high-resolution images of human faces. It contains 70k images with an original resolution of  $1024 \times 1024$ , which we resize to  $128 \times 128$ . Finally, LSUN Bedroom is a dataset of  $\sim 3$  million images of bedrooms with varying resolutions. We resize all LSUN Bedroom images to  $128 \times 128$  and  $256 \times 256$  and evaluate models on both resolutions.

To assess the performance of image generation models, we adopt the Fréchet Inception Distance (FID) [43]. In this metric, the distance between visual features of the real data distribution and the generated data distribution is computed, where the visual features are obtained by encoding the images with a pre-trained Inception-v3 network [44]. Unlike FID, the spatial FID (sFID) captures spatial relationships by employing spatial features rather than standard pooled features. In addition to FID and sFID, we also report Precision and Inception Score (IS) to measure the fidelity of the generated samples and Recall to measure their diversity. Since FID is sensitive to the size of both the real data and the generated data, we follow the same evaluation methodology as previous works for the sake of comparison. Specifically, similar to ViTGAN [7], we compute the FID between all the training images and 50k generated images for CIFAR-10 and between the test images and 19,962 generated images for CelebA. Given the large number of training images in LSUN Bedroom, we calculate the FID between 50k randomly sampled training images and 50k generated images, as done by Ho et al. [4]. Finally, like ADM-IP [6], we compute the FID between 50k

randomly selected training images and the complete training set for FFHQ. Additionally, we evaluate the complexity of the models in terms of FLOPs, parameters, throughput, and images observed during training.

### B. Implementation details

We train all models with  $R_1$  regularization [39] and the Adam optimizer [45] with  $\beta_1 = 0.5$  and  $\beta_2 = 0.99$ . For all resolutions, the generator learning rate is 0.0002. For the convolutional discriminators, the learning rate is 0.0004, while for the Transformer discriminators, we set it to 0.0002. We use convolutional discriminators for all experiments in subsection IV-C. The initial Ladaformer block generates  $8 \times 8$  maps with dimension 1024, followed by a  $16 \times 16$  Ladaformer with dimension 256. The last Ladaformer generates maps of  $32 \times 32$  with dimension 64. For CIFAR-10, we use pixel-level generation. For CelebA we use patch generation. On the other hand, for FFHQ and LSUN bedroom we stack a convolutional decoder with upsampling in the final Ladaformer block instead of performing patch or pixel generation. The number of heads is 4, and the MLP dimension is 512 in all Ladaformers. For CIFAR-10 and FFHQ we use Translation, Color, and Cutout data augmentation [46], and a balanced consistency regularization (bCR) [47] with  $\lambda_{real} = \lambda_{fake} = 1.0$  and 0.1 respectively. For CelebA and LSUN bedroom we use Translation and Color data augmentation and do not employ bCR since we do not observe a performance gain.

### C. Ablation studies

We evaluate the image generation quality, efficiency and stability of a Ladaformer generator and compare it with Linformer low-rank attention, Swin-Transformer down-sampling attention, and Fastformer original additive attention. In addition, we evaluate Ladaformer with a Swin-style down-sampling technique, which we call Lada-Swin. We carry out an ablation study to analyze the stability and compatibility of generators based on these attention mechanisms with a

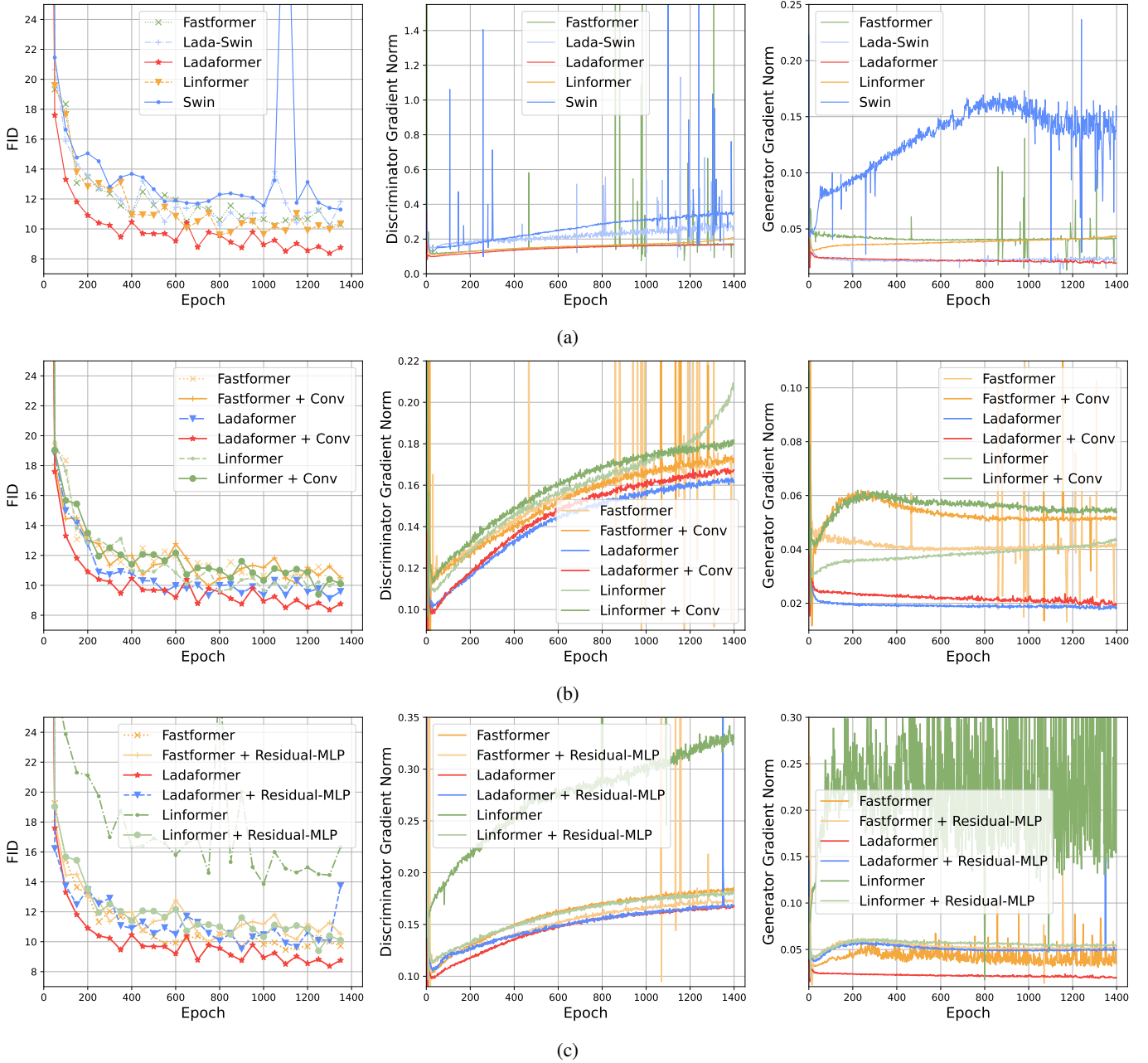


Fig. 5: Gradient magnitudes over all parameters of the LadaGAN generator and discriminator, and FID evaluation of the attention mechanisms (a), convolutional layer (b), and MLP residual connection (c).

convolutional layer and the residual connection of the MLP. We also examine the impact of the self-modulated layer normalization on the Ladaformer performance. To make the models comparable, we use the same training configuration (see IV-B) and set some of the hyperparameters so that all generators take approximately the same number of FLOPs. In particular, all Fastformer hyperparameters are the same as Ladaformer, whereas for Linformer, we use a  $k = 64$  and for Swin Transformer and Lada-Swin, a window size of  $8 \times 8$ . For all configurations, we employ a convolutional discriminator identical to FastGAN discriminator but without batch normalization. The main block of this architecture consists of a convolutional residual block with an average pool residual

connection (similar to the green blocks in Figure 4).

Table I shows the FID scores, IS Precision, Recall, and number of FLOPs for all the evaluated attention mechanisms and configurations. As can be observed, the Ladaformer with a convolutional layer and without the residual connection achieves the best evaluation with a similar number of FLOPs. In general, adding a convolutional layer has a positive effect on Ladaformer, a negative effect for Linformer and practically no effect for Fastformer. This shows not only that the combination of Ladaformer and convolutions does not lead to training instabilities, but also that it can provide noticeable benefits for the quality of the generated images. This is because the locality of the convolutional layer might complement the long-range

TABLE II: FID and number of FLOPs for ConvNet and Ladaformer discriminators with and without LEE on CIFAR-10 ( $32 \times 32$ ), CelebA ( $64 \times 64$ ) and LSUN Bedroom ( $128 \times 128$ ).

Dataset	D-type	D-lr	LEE	G-emb sizes	G-FLOPs	D-FLOPs	FID ↓	sFID ↓	IS ↑	Prec ↑	Rec ↑
CIFAR-10	Conv <sup>†</sup>	0.0002	✗	{1024, 256, 64}	0.7B	0.5B	4.72	4.44	9.36	0.59	0.57
	Conv <sup>†</sup>	0.0002	✓	{1024, 256, 128}	0.9B	0.5B	4.68	4.51	9.50	0.59	0.55
	Lada <sup>†</sup>	0.0002	✗	{1024, 256, 64}	0.7B	0.7B	<b>3.29</b>	3.81	<b>9.66</b>	<b>0.61</b>	<b>0.60</b>
	Lada <sup>†</sup>	0.0002	✓	{1024, 256, 128}	0.9B	0.7B	3.60	<b>3.80</b>	9.54	0.60	<b>0.60</b>
CelebA	Conv	0.0004	✗	{1024, 256, 64}	0.7B	0.7B	3.43	11.98	3.31	<b>0.67</b>	0.55
	Conv	0.0004	✓	{1024, 256, 128}	0.9B	0.7B	3.36	11.79	<b>3.36</b>	0.66	0.58
	Lada	0.0002	✗	{1024, 256, 64}	0.7B	0.9B	<b>2.89</b>	11.24	3.26	<b>0.67</b>	0.58
	Lada	0.0002	✓	{1024, 256, 128}	0.9B	0.9B	3.04	<b>11.16</b>	3.26	<b>0.67</b>	<b>0.59</b>
LSUN Bedroom *	Conv	0.0004	✗	{1024, 256, 64}	0.9B	0.9B	9.33	24.40	<b>2.27</b>	0.43	0.29
	Conv	0.0004	✓	{1024, 512, 256}	4.3B	0.9B	5.82	15.17	2.25	0.49	0.36
	Lada	0.0002	✗	{1024, 256, 64}	0.9B	1.1B	6.46	20.35	2.14	0.45	0.38
	Lada	0.0002	✓	{1024, 512, 256}	4.3B	1.1B	<b>4.60</b>	<b>14.81</b>	2.22	<b>0.52</b>	<b>0.41</b>

\* Convolutional decoder with nearest neighbor upsampling instead of patch generation.

† With bCR regularization.

dependencies of the additive attention map that is propagated by the element-wise operation in equation 3. Note that, as opposed to Lada, Fastformer attention mechanism compresses the representation by computing a second additive attention map for the keys instead of propagating it through an element-wise operation, which seems to prevent the benefits of the convolutional layer.

Interestingly, Fastformer and Ladaformer obtained slightly lower FIDs without the residual connection. However, when Ladaformer employs SLN, the improvement in the FID when removing this connection is stronger. On the other hand, the performance of Linformer, which is built upon dot-product attention, deteriorates considerably when removing the residual connection. This suggests that Transformers based on linear additive attention mechanisms are less dependent on such shortcuts to propagate the gradients properly and that SLN might be playing a similar role in these kinds of connections. However, this behavior indicates that more investigation is required into the residual connections and modulation of Transformers that do not employ dot-product attention.

Moreover, we analyze the gradients in both the convolutional discriminator and the attention-based generator during training. Figure 5 depicts the FID and gradient norms of all the evaluated Transformers with and without convolutions and residual connections for each epoch. As can be observed, the Swin-Transformer configuration exhibits considerably larger gradient norms in the generator compared to the rest of the attention mechanisms, while Lada and Lada-Swin have the smallest norms. On the other hand, all attention mechanisms have similar gradient norms in the discriminator, although Fastformer, Swin, and Lada-Swin present several large gradient spikes. Remarkably, Lada and Linformer show stable training with no gradient spikes, leading to the lowest FIDs. This highlights the importance of controlling gradient norms in both the generator and discriminator. Moreover, the gradient behavior seems to be associated with the specific architecture of the Transformer generator.

Although Swin-Transformer has consistently shown state-of-the-art performance in different applications, in our experiments it obtains the highest FIDs. This is consistent

with [7] that reports inferior FID when employing Swin-Transformers in the generator. Notably, Lada-Swin outperforms Swin-Transformer and overcomes the generator gradient spikes while reducing those of the discriminator. This suggests that the dot-product windows are a possible source of such gradient behavior and that it can be mitigated with Lada.

The effect of the residual connection on the gradients of Linformer and Fastformer can be seen in Figure 5. Removing the residual connection considerably increases the gradient norms of Linformer in both the generator and discriminator, while the gradients in the generator become widely unstable. In contrast, although removing the residual connection in LadaGAN leads to slightly higher FIDs and larger gradient norms, in general they remain stable. This is in part because of the  $R_1$  penalty and its compatibility with LadaGAN, as discussed in subsection IV-C. Note that these effects are not observed when adding or removing the convolutional layer (see Figure 5).

These results demonstrate that even slight differences in the attention mechanism can lead to instabilities. That is the case with Fastformer and LadaGAN: despite having a similar architecture, the former has multiple and larger gradient spikes while the latter is significantly more stable. Moreover, down-sampling Lada attention in the same way as Swin-Transformer (i.e. Lada-Swin) results in larger norms and some gradient spikes, albeit smaller than Fastformer and Swin-Transformer (i.e. down-sampling the dot-product attention).

#### D. Lada discriminator

Using Transformers in the discriminator of GANs has been particularly challenging because regularization techniques such as  $R_1$  gradient penalty often lead to unstable training [7]. Although there are some notable exceptions to this (e.g. [7], [17]), they require laborious engineering and rarely outperform ConvNets. For this reason, most Transformer-based GANs employ ConvNet discriminators. In this context, we study the stability of Ladaformer discriminators trained with  $R_1$  gradient penalty compared to ConvNet discriminators, as well as the impact of increasing the model size with LEE.

TABLE III: FID scores for CIFAR-10 models trained using 100%, 20%, and 10% of images, computed with 50k training images and 10k test images. \*Results from [46] and [7].

Method	100% data		20% data		10% data	
	50k	10k	50k	10k	50k	10k
VITGAN [7]	6.66*	-	-	-	-	-
w/o. bCR	8.84*	-	-	-	-	-
StyleGAN2 [11]	5.79*	9.89*	-	12.15*	-	14.50*
LadaGAN	<b>3.29</b>	<b>7.58</b>	<b>6.85</b>	<b>11.06</b>	<b>8.93</b>	<b>12.97</b>
w/o. bCR	4.88	9.01	10.67	15.09	12.79	16.84

Table II shows the FIDs obtained with different configurations of ConvNet and Ladaformer discriminators on CIFAR-10, CelebA and LSUN Bedroom. In addition, the number of FLOPs for the discriminator and generator, as well as the sizes of the embeddings in the generator corresponding to the three Ladaformer blocks in Figure 4, are also presented. As can be observed, the Ladaformer discriminators consistently outperform convolutional discriminators. However, the difference is small for CIFAR-10 and CelebA and significantly larger for LSUN Bedroom where larger generators are employed. Interestingly, a higher learning rate is required for the convolutional discriminator to match the Ladaformer discriminator FID. We also observe that, in LSUN Bedroom, using LEE leads to the lowest FID, while in CIFAR-10 and CelebA LEE does not make any difference. We hypothesize that this behavior is due to the resolution of the dataset, since high-resolution images require larger models. Note that in the LSUN Bedroom experiment, the Ladaformer blocks of the generator increase their embedding dimension locally from  $\{1024, 256, 64\}$  to  $\{1024, 512, 256\}$ , which in turn increases the number of FLOPs.

### E. Data efficiency

To analyze the behavior of LadaGAN under small-data regimes, we conducted experiments on CIFAR-10 with different training data sizes. In Table III, the FID scores of LadaGAN and StyleGAN2 with 10%, 20%, and 100% of training data are reported. As can be observed, LadaGAN outperforms StyleGAN2 in all scenarios without any hyperparameter changes. Moreover, LadaGAN with 20% of training data achieves a FID score relatively similar to StyleGAN2 with 100% of training data in both 50k and 10k evaluations. Note that since previous works compute the FID on CIFAR-10 using 10k sampled images (e.g. [46]) and we compute it using 50k sampled images, the results are not comparable. Therefore, we compute the FID scores using both 50k and 10k images and present them in Table III.

Additionally, we conducted experiments without regularization. The results indicate that StyleGAN2 with just 5% outperforms LadaGAN without bCR. However, as the dataset size increases, LadaGAN consistently surpasses StyleGAN2 in terms of FID, even without bCR. These results show that LadaGAN is a suitable architecture for large datasets.

### F. Comparison with state-of-the-art models

We compare LadaGAN FID scores on CIFAR-10, CelebA, FFHQ, and LSUN Bedroom at two different resolutions with state-of-the-art single-step and multi-step image generation models. For a fair comparison, in addition to the evaluation described in subsection IV-B, we compute FID scores following VITGAN, SS-GAN, ADM-IP, and CT. More specifically, for CelebA, we compute the FID score between 19,962 generated samples and the 19,962 test images and also between 50k generated samples and the whole training set. For LSUN Bedroom  $128 \times 128$ , we compute FID between 30k randomly sampled images and 30k generated images. For LSUN Bedroom  $256 \times 256$ , we generate 50k images and use the same reference distribution statistics as CT, which was computed over 50k training samples. Consequently, we also apply the same data preprocessing for training such LadaGAN model.

We leave the integration of LadaGAN with adaptive discriminator augmentation methods for future work, as these variants [48], [49] require further hyperparameter tuning. The resulting configurations could then be compared to models such as StyleGAN2-ADA [48], Styleformer [50], and Diffusion-GAN [49]. In this work, to ensure a fair evaluation of the proposed architecture, our current comparison is limited to models that utilize differentiable augmentation.

Table IV shows the reported FID scores for StyleGAN2, BigGAN, Vanilla-ViT, ViTGAN, TransGAN, a combination of StyleGAN2 and ViTGAN, as well as CT with 1 and 2 sampling steps and ADM-IP with 80 and 1000 sampling steps. Notably, LadaGAN outperforms state-of-the-art convolutional and Transformer GANs and CT in all datasets and resolutions. Moreover, LadaGAN achieves competitive performance compared to ADM with 80 sampling steps and even to ADM with 1000 sampling steps, despite being a single-step generation method.

On the other hand, we compare LadaGAN efficiency with state-of-the-art image generation models in terms of model size and complexity. Table V reports the number of parameters, FLOPs, throughput, and the number of images seen during training for LadaGAN, ViTGAN, StyleGAN2, CT, and ADM-IP with different image resolutions. For all datasets and resolutions, LadaGAN required the least number of parameters and FLOPs. In particular, LadaGAN required significantly fewer FLOPs: only 8.9% FLOPs of StyleGAN2 and 26.9% of ViTGAN for the  $64 \times 64$  resolution, and  $\sim 37.5\%$  for the  $128 \times 128$  resolution. As expected, despite reducing the number of sampling steps, the number of FLOPs and throughput required for the multi-step generation models ADM-IP and CT is orders of magnitude higher than GANs, which are single-step generators. Note that although for the  $32 \times 32$  resolution ADM-IP and LadaGAN require almost the same number of images during training, when the resolution increases ( $64 \times 64$ ) LadaGAN requires approximately half the images of ADM-IP. Finally, we find that CT has significantly more parameters than LadaGAN and is the model that requires to train longer.

Remarkably, in contrast to ADM-IP which drastically increases the number of parameters and FLOPs for higher resolutions, LadaGAN parameters and FLOPs remain practically

TABLE IV: Comparison with state-of-the-art models. FID for CIFAR-10 with 50k samples, CelebA with 19k and 50k samples, FFHQ with 70k samples, and LSUN Bedroom with 30k and 50k samples. \*Results from the original papers.

Method		CIFAR 10	CelebA		FFHQ	LSUN	LSUN
		32x32	64x64	64x64	128x128	128x128	256x256
		50k	19k	50k	50k	30k	50k
Single-step	SS-GAN [51]	15.60*	-	-	-	13.30*	-
	TransGAN [17]	9.02*	-	-	-	-	-
	Vanilla-ViT [7]	12.70*	20.20*	-	-	-	-
	VITGAN [7]	4.92*	3.74*	-	-	-	-
	GANformer [24]	-	-	-	-	-	6.51*
	BigGAN + DiffAugment [46]	4.61*	-	-	-	-	-
	StyleGAN2 + DiffAugment [46]	5.79*	-	-	-	-	-
	StyleGAN2-D + ViTGAN-G [7]	4.57*	-	-	-	-	-
	CT [33]	8.70*	-	-	-	-	16.0*
	LadaGAN	<b>3.29</b>	<b>2.89</b>	<b>1.81</b>	<b>4.48</b>	<b>5.08</b>	<b>6.36</b>
Multi-step	CT (2 steps) [33]	5.83*	-	-	-	-	7.85*
	ADM-IP (80 steps) [6]	2.93*	-	2.67*	6.89*	-	-
	ADM-IP (1000 steps) [6]	<b>2.76*</b>	-	<b>1.31*</b>	<b>2.98*</b>	-	-

TABLE V: Computation cost for 80 ADM-IP steps and 2 CT steps. For CelebA ( $64 \times 64$ ), LadaGAN is trained on a single NVIDIA 3080 Ti GPU in less than 35 hours, while ADM training takes 5 days on 16 Tesla V100 GPUs. \*Results from [7]. †Results from [46].

Resolution		CT [33]	ADM-IP [6]	StyleGAN2 [11]	VITGAN [7]	LadaGAN
32 <sup>2</sup>	#Params	-	57M	-	-	<b>19M</b>
	FLOPs	-	9.0B	-	-	<b>0.7B</b>
	#Images	409M	69M	200M <sup>†</sup>	-	<b>68M</b>
	Throughput (images / sec)	-	0.66	-	-	<b>416.66</b>
64 <sup>2</sup>	#Params	-	295M	24M*	38M*	<b>19M</b>
	FLOPs	-	103.5B	7.8B*	2.6B*	<b>0.7B</b>
	#Images	-	138M	-	-	<b>72M</b>
	Throughput (images / sec)	-	0.50	-	-	<b>333.33</b>
128 <sup>2</sup>	#Params	-	543M	-	-	<b>24M</b>
	FLOPs	-	391.0B	11.5B*	11.8B*	<b>4.3B</b>
	#Images	-	61M	-	-	<b>53M</b>
	Throughput (images / sec)	-	0.23	-	-	<b>192.30</b>
256 <sup>2</sup>	#Params	526M	-	-	-	<b>24M</b>
	FLOPs	-	-	15.2B*	52.1B*	<b>5.5B</b>
	#Images	2048M	-	-	-	<b>18M</b>
	Throughput (images / sec)	4.18	-	-	-	<b>63.69</b>

the same between  $32 \times 32$  and  $64 \times 64$ ; this is because instead of generating pixels, the final Ladaformer block generates patches of  $2 \times 2$ , resulting in almost the same architecture.

### G. Generated images and interpolation

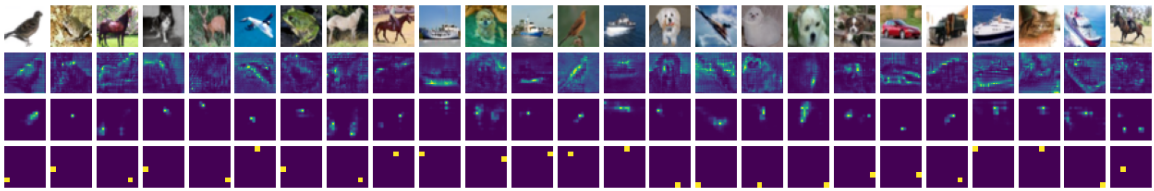
In addition to the FID-based evaluation, we visually inspect sampled images for a qualitative evaluation. In Figure 6, we present curated images generated by the best performing LadaGAN models for CIFAR-10, CelebA, FFHQ and LSUN bedrooms (see Table II), together with associated attention maps at the  $8 \times 8$ ,  $16 \times 16$ , and  $32 \times 32$  stages, which correspond to the three Ladaformer blocks in Figure 4. In general, we observe that LadaGAN models can generate realistic-looking and diverse images for all datasets. In particular, the images generated by the CIFAR-10 model represent different categories, viewpoints, backgrounds, and even variations within some categories; the CelebA and FFHQ models generate face images with different genres, ethnicities, ages, hairstyles, clothing,

viewpoints, and backgrounds; and the LSUN bedroom images contain different styles, colors, and decorations. Interestingly, the  $8 \times 8$  attention maps resemble access to a single token, whereas the  $16 \times 16$  and  $32 \times 32$  maps generate a global structure of the image. Note that for CIFAR-10 and LSUN bedroom the  $16 \times 16$  maps also seem to converge to a single token, similar to the  $8 \times 8$  maps, but for FFHQ and CelebA the global structure appears to be preserved. Moreover, as shown in Figure 7, LadaGAN models generate realistic images and smooth transitions of linearly interpolated latent vectors.

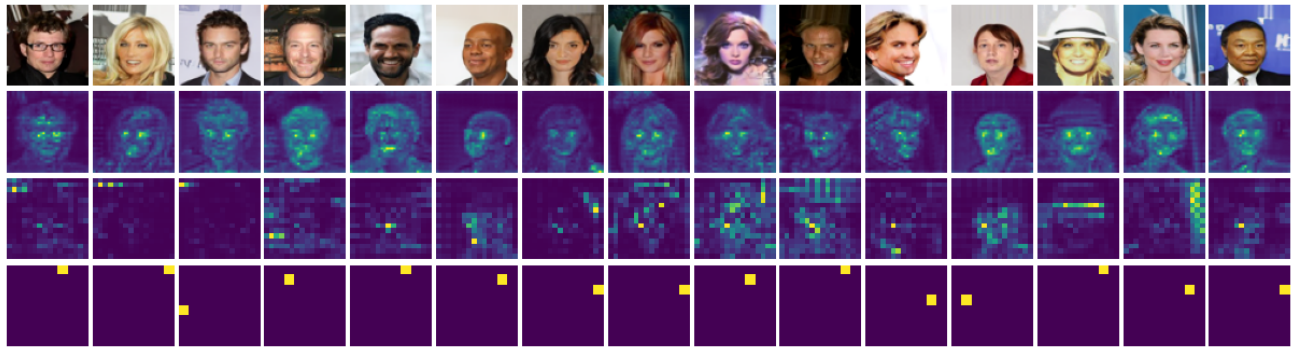
## V. CONCLUSION

In this paper, we presented LadaGAN, an efficient GAN architecture based on a novel linear additive-attention block called Ladaformer. This block showed to be more suitable for both the generator and the discriminator than other efficient Transformer blocks, allowing stable GAN training in different scenarios. Our findings indicate that Ladaformer

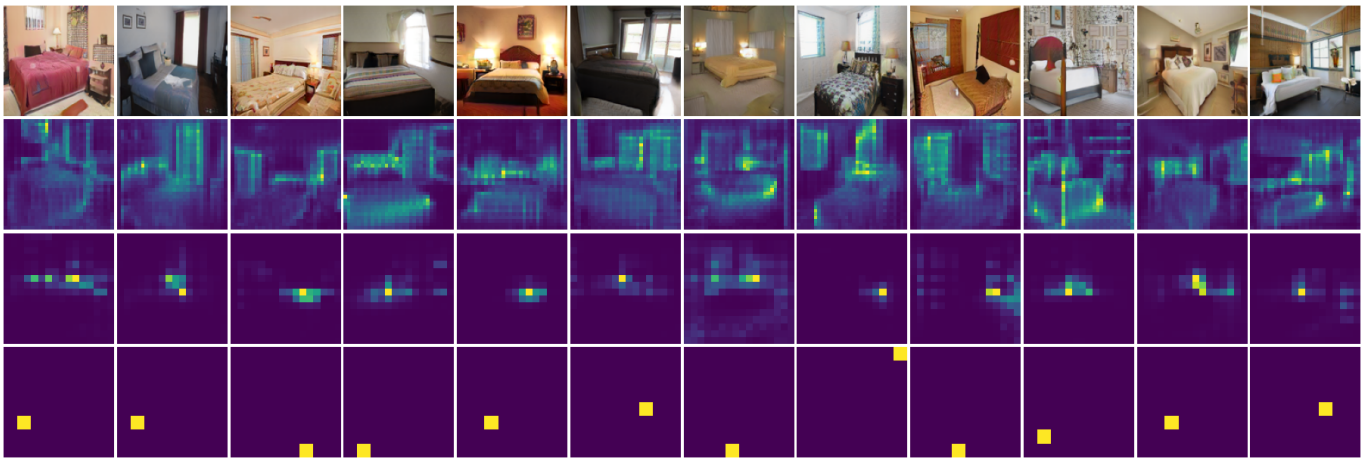




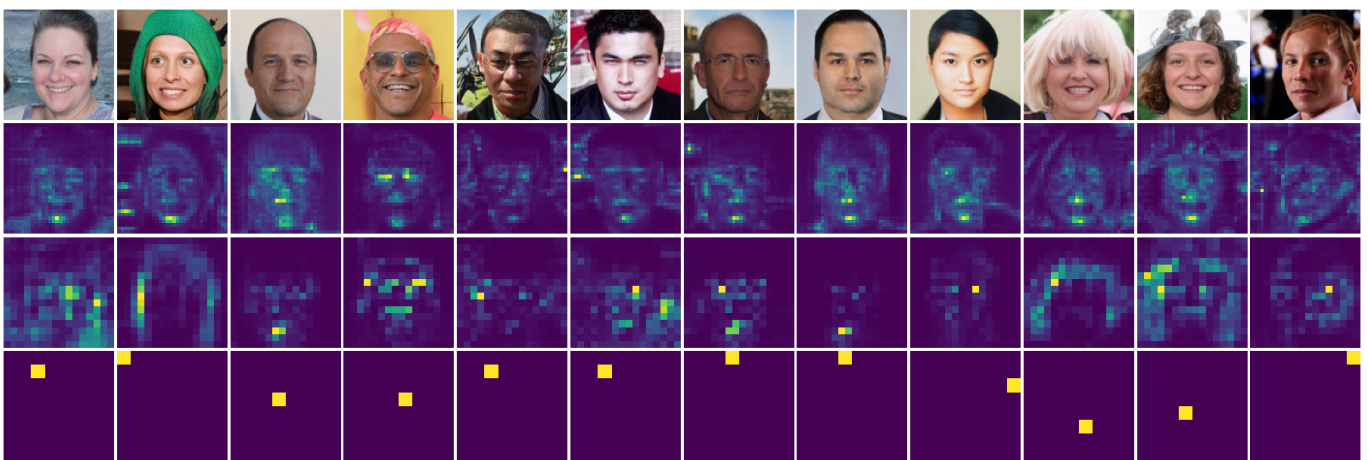
(a)



(b)



(c)



(d)

Fig. 6: Samples from LadaGAN models on CIFAR-10 (a), CelebA (b), LSUN Bedroom (c), and FFHQ (d), along with corresponding additive attention maps for a single head from the  $32 \times 32$ ,  $16 \times 16$ , and  $8 \times 8$  Ladaformer blocks.

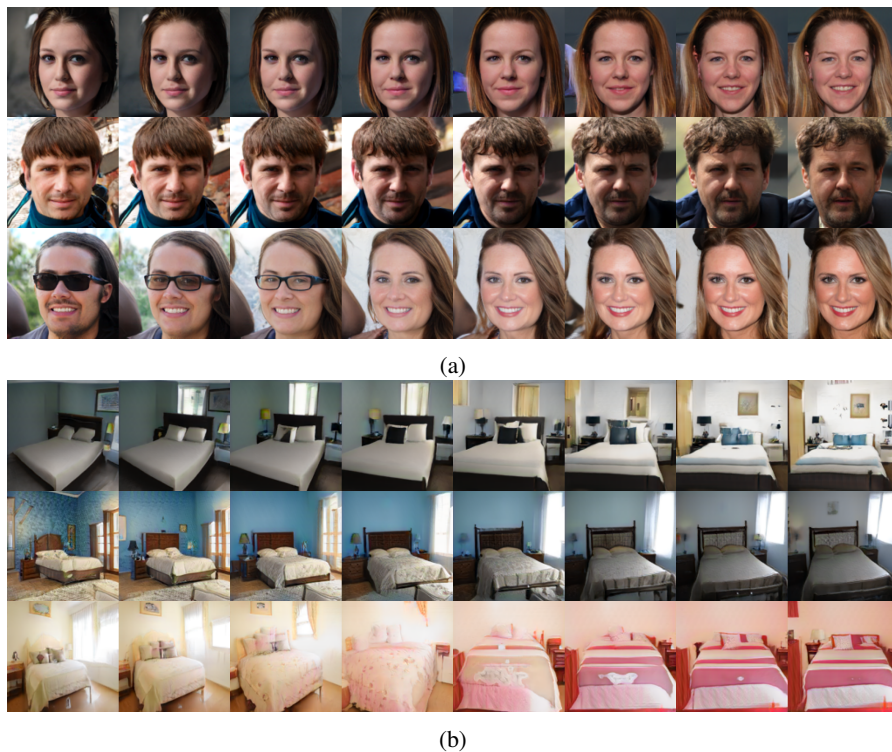


Fig. 7: Latent space interpolations with LadaGAN models for a) FFHQ and b) LSUN Bedroom.

is convolution-compatible and LadaGAN is gradient-stable and highly effective for image generation tasks. Remarkably, LadaGAN outperformed ConvNet and Transformer GANs on multiple benchmark datasets at different resolutions while requiring significantly fewer FLOPs. Moreover, compared with diffusion models and Consistency Training, LadaGAN achieves competitive performance at a fraction of the computational cost.

To the best of our knowledge, LadaGAN is the first GAN architecture based on linear additive-attention mechanisms. Therefore, our results provide further evidence of the efficiency and expressive power of linear attention-mechanisms and open the door for future research on efficient GAN architectures with a performance similar to modern diffusion models. We believe LadaGAN can help laboratories and research groups to perform experiments faster with limited computing budgets, advancing the applications of generative models without losing quality while reducing energy consumption and minimizing the carbon footprint.

As future work, we plan to train LadaGAN in audio and text-to-image scenarios. Moreover, the Ladaformer block and its compatibility with convolutions remain to be explored in other tasks, like image and video classification.

#### ACKNOWLEDGEMENTS

Emilio Morales-Juarez was supported by the National Council for Science and Technology (CONACYT), Mexico, scholarship number 782143.

#### REFERENCES

- [1] I. Goodfellow, J. Pouget-Abadie, M. Mirza, B. Xu, D. Warde-Farley, S. Ozair, A. Courville, and Y. Bengio, “Generative adversarial nets,” in *Advances in neural information processing systems*, 2014, pp. 2672–2680.
- [2] A. Sauer, K. Schwarz, and A. Geiger, “Stylegan-xl: Scaling stylegan to large diverse datasets,” in *ACM SIGGRAPH 2022 Conference Proceedings*, 2022, pp. 1–10.
- [3] R. Mokady, O. Tov, M. Yarom, O. Lang, I. Mosseri, T. Dekel, D. Cohen-Or, and M. Irani, “Self-distilled stylegan: Towards generation from internet photos,” in *ACM SIGGRAPH 2022 Conference Proceedings*, 2022, pp. 1–9.
- [4] J. Ho, A. Jain, and P. Abbeel, “Denoising diffusion probabilistic models,” *Advances in Neural Information Processing Systems*, vol. 33, pp. 6840–6851, 2020.
- [5] T. Salimans and J. Ho, “Progressive distillation for fast sampling of diffusion models,” *arXiv preprint arXiv:2202.00512*, 2022.
- [6] M. Ning, E. Sangineto, A. Porrello, S. Calderara, and R. Cucchiara, “Input perturbation reduces exposure bias in diffusion models,” *arXiv preprint arXiv:2301.11706*, 2023.
- [7] K. Lee, H. Chang, L. Jiang, H. Zhang, Z. Tu, and C. Liu, “Vitgan: Training gans with vision transformers,” in *International Conference on Learning Representations*, 2021.
- [8] M. Arjovsky, S. Chintala, and L. Bottou, “Wasserstein generative adversarial networks,” in *ICML*, 2017.
- [9] T. Miyato, T. Kataoka, M. Koyama, and Y. Yoshida, “Spectral normalization for generative adversarial networks,” in *ICLR*, 2018.
- [10] T. Karras, S. Laine, and T. Aila, “A style-based generator architecture for generative adversarial networks,” in *Proceedings of the IEEE conference on computer vision and pattern recognition*, 2019, pp. 4401–4410.
- [11] T. Karras, S. Laine, M. Aittala, J. Hellsten, J. Lehtinen, and T. Aila, “Analyzing and improving the image quality of stylegan,” in *Proceedings of the IEEE/CVF Conference on Computer Vision and Pattern Recognition*, 2020, pp. 8110–8119.
- [12] A. Dosovitskiy, L. Beyer, A. Kolesnikov, D. Weissenborn, X. Zhai, T. Unterthiner, M. Dehghani, M. Minderer, G. Heigold, S. Gelly, J. Uszkoreit, and N. Houlsby, “An image is worth 16x16 words: Transformers for image recognition at scale,” in *ICLR*, 2021.
- [13] A. Vaswani, N. Shazeer, N. Parmar, J. Uszkoreit, L. Jones, A. N. Gomez, L. Kaiser, and I. Polosukhin, “Attention is all you need,” *Advances in neural information processing systems*, vol. 30, 2017.
- [14] B. Zhang, S. Gu, B. Zhang, J. Bao, D. Chen, F. Wen, Y. Wang, and B. Guo, “Stylewin: Transformer-based gan for high-resolution image

- generation,” in *Proceedings of the IEEE/CVF Conference on Computer Vision and Pattern Recognition*, 2022, pp. 11 304–11 314.
- [15] C. Wu, F. Wu, T. Qi, Y. Huang, and X. Xie, “Fastformer: Additive attention can be all you need,” *arXiv preprint arXiv:2108.09084*, 2021.
- [16] A. Brock, J. Donahue, and K. Simonyan, “Large scale gan training for high fidelity natural image synthesis,” in *ICLR*, 2019.
- [17] Y. Jiang, S. Chang, and Z. Wang, “Transgan: Two transformers can make one strong gan,” *arXiv preprint arXiv:2102.07074*, 2021.
- [18] I. Gulrajani, F. Ahmed, M. Arjovsky, V. Dumoulin, and A. C. Courville, “Improved training of wasserstein gans,” in *Advances in neural information processing systems*, 2017, pp. 5767–5777.
- [19] Y. Xiong, Z. Zeng, R. Chakraborty, M. Tan, G. Fung, Y. Li, and V. Singh, “Nyströmformer: A nyström-based algorithm for approximating self-attention,” in *Proceedings of the AAAI Conference on Artificial Intelligence*, vol. 35, no. 16, 2021, pp. 14 138–14 148.
- [20] M. Kumar, D. Weissenborn, and N. Kalchbrenner, “Colorization transformer,” *arXiv preprint arXiv:2102.04432*, 2021.
- [21] H. Kim, G. Papamakarios, and A. Mnih, “The lipschitz constant of self-attention,” in *International Conference on Machine Learning*. PMLR, 2021, pp. 5562–5571.
- [22] I. Anokhin, K. Demochkin, T. Khakhulin, G. Sterkin, V. Lempitsky, and D. Korzhnikov, “Image generators with conditionally-independent pixel synthesis,” in *Proceedings of the IEEE/CVF Conference on Computer Vision and Pattern Recognition*, 2021, pp. 14 278–14 287.
- [23] X. Zhai, A. Kolesnikov, N. Houlsby, and L. Beyer, “Scaling vision transformers,” in *Proceedings of the IEEE/CVF Conference on Computer Vision and Pattern Recognition*, 2022, pp. 12 104–12 113.
- [24] D. A. Hudson and L. Zitnick, “Generative adversarial transformers,” in *International conference on machine learning*. PMLR, 2021, pp. 4487–4499.
- [25] H. Touvron, M. Cord, A. El-Nouby, P. Bojanowski, A. Joulin, G. Synnaeve, and H. Jégou, “Augmenting convolutional networks with attention-based aggregation,” *arXiv preprint arXiv:2112.13692*, 2021.
- [26] H. Wu, B. Xiao, N. Codella, M. Liu, X. Dai, L. Yuan, and L. Zhang, “Cvt: Introducing convolutions to vision transformers,” in *Proceedings of the IEEE/CVF International Conference on Computer Vision*, 2021, pp. 22–31.
- [27] N. Park and S. Kim, “How do vision transformers work?” in *International Conference on Learning Representations*, 2021.
- [28] J. Sohl-Dickstein, E. Weiss, N. Maheswaranathan, and S. Ganguli, “Deep unsupervised learning using nonequilibrium thermodynamics,” in *International conference on machine learning*. PMLR, 2015, pp. 2256–2265.
- [29] J. Song, C. Meng, and S. Ermon, “Denoising diffusion implicit models,” *arXiv preprint arXiv:2010.02502*, 2020.
- [30] A. Q. Nichol and P. Dhariwal, “Improved denoising diffusion probabilistic models,” in *International Conference on Machine Learning*. PMLR, 2021, pp. 8162–8171.
- [31] P. Dhariwal and A. Nichol, “Diffusion models beat gans on image synthesis,” *Advances in Neural Information Processing Systems*, vol. 34, pp. 8780–8794, 2021.
- [32] T. Karras, M. Aittala, T. Aila, and S. Laine, “Elucidating the design space of diffusion-based generative models,” *Advances in Neural Information Processing Systems*, vol. 35, pp. 26 565–26 577, 2022.
- [33] Y. Song, P. Dhariwal, M. Chen, and I. Sutskever, “Consistency models,” *arXiv preprint arXiv:2303.01469*, 2023.
- [34] D. Bahdanau, K. Cho, and Y. Bengio, “Neural machine translation by jointly learning to align and translate,” *arXiv preprint arXiv:1409.0473*, 2014.
- [35] T. Chen, M. Lucic, N. Houlsby, and S. Gelly, “On self modulation for generative adversarial networks,” in *ICLR*, 2019. [Online]. Available: <https://openreview.net/forum?id=Hk15aoR5tm>
- [36] B. Liu, Y. Zhu, K. Song, and A. Elgammal, “Towards faster and stabilized gan training for high-fidelity few-shot image synthesis,” in *International Conference on Learning Representations*, 2020.
- [37] S. Ioffe and C. Szegedy, “Batch normalization: Accelerating deep network training by reducing internal covariate shift,” in *International conference on machine learning*. PMLR, 2015, pp. 448–456.
- [38] J. Devlin, M.-W. Chang, K. Lee, and K. Toutanova, “Bert: Pre-training of deep bidirectional transformers for language understanding,” in *ACL*, 2019.
- [39] L. Mescheder, A. Geiger, and S. Nowozin, “Which training methods for gans do actually converge?” in *International conference on machine learning*. PMLR, 2018, pp. 3481–3490.
- [40] A. Krizhevsky, “Learning multiple layers of features from tiny images,” University of Toronto, Tech. Rep., April 2009.
- [41] Z. Liu, P. Luo, X. Wang, and X. Tang, “Deep learning face attributes in the wild,” in *Proceedings of International Conference on Computer Vision (ICCV)*, December 2015.
- [42] F. Yu, Y. Zhang, S. Song, A. Seff, and J. Xiao, “Lsun: Construction of a large-scale image dataset using deep learning with humans in the loop,” *arXiv preprint arXiv:1506.03365*, 2015.
- [43] M. Heusel, H. Ramsauer, T. Unterthiner, B. Nessler, and S. Hochreiter, “Gans trained by a two time-scale update rule converge to a local nash equilibrium,” *Advances in neural information processing systems*, vol. 30, 2017.
- [44] C. Szegedy, V. Vanhoucke, S. Ioffe, J. Shlens, and Z. Wojna, “Rethinking the inception architecture for computer vision,” in *Proceedings of the IEEE conference on computer vision and pattern recognition*, 2016, pp. 2818–2826.
- [45] D. P. Kingma and J. Ba, “Adam: A method for stochastic optimization,” *arXiv preprint arXiv:1412.6980*, 2014.
- [46] S. Zhao, Z. Liu, J. Lin, J.-Y. Zhu, and S. Han, “Differentiable augmentation for data-efficient gan training,” in *NeurIPS*, 2020.
- [47] L. Zhao, Z. Zhang, T. Chen, D. Metaxas, and H. Zhang, “Improved transformer for high-resolution gans,” *Advances in Neural Information Processing Systems*, vol. 34, 2021.
- [48] T. Karras, M. Aittala, J. Hellsten, S. Laine, J. Lehtinen, and T. Aila, “Training generative adversarial networks with limited data,” in *Proc. NeurIPS*, 2020.
- [49] Z. Wang, H. Zheng, P. He, W. Chen, and M. Zhou, “Diffusion-gan: Training gans with diffusion,” *International Conference on Learning Representations*, 2023.
- [50] J. Park and Y. Kim, “Styleformer: Transformer based generative adversarial networks with style vector,” in *Proceedings of the IEEE/CVF conference on computer vision and pattern recognition*, 2022, pp. 8983–8992.
- [51] T. Chen, X. Zhai, M. Ritter, M. Lucic, and N. Houlsby, “Self-supervised gans via auxiliary rotation loss,” in *Proceedings of the IEEE/CVF conference on computer vision and pattern recognition*, 2019, pp. 12 154–12 163.